JACS
JOURNAL OF THE AMERICAN CHEMICAL SOCIETY

Article

Dramatic Influence of the Orientation of Linker between Hydrophilic and Hydrophobic Lipid Moiety in Liposomal Gene Delivery

Mukthavaram Rajesh, Joyeeta Sen, Marepally Srujan,
Koushik Mukherjee, Bojja Sreedhar, and Arabinda Chaudhuri

J. Am. Chem. Soc., **2007**, 129 (37), 11408-11420• DOI: 10.1021/ja0704683 • Publication Date (Web): 25 August 2007

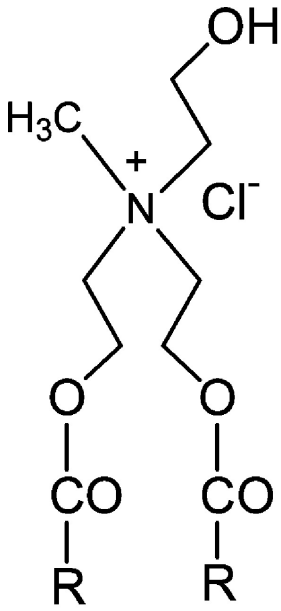

Lipid 1

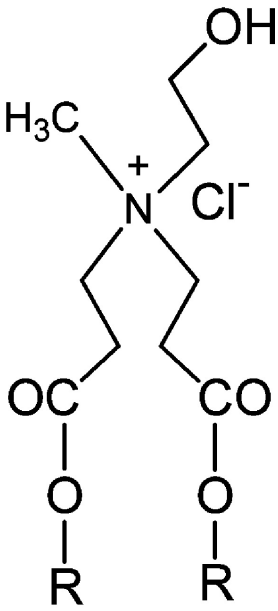

Lipid 2

$$R = n\text{-}C_{13}H_{27}$$

More About This Article

Additional resources and features associated with this article are available within the HTML version:

- Supporting Information

J|A|C|S
ARTICLES
Published on Web 08/25/2007

Dramatic Influence of the Orientation of Linker between Hydrophilic and Hydrophobic Lipid Moiety in Liposomal Gene Delivery

Mukthavaram Rajesh,[†] Joyeeta Sen,[†,§] Marepally Srujan,[†] Koushik Mukherjee,[†,||] Bojja Sreedhar,[‡] and Arabinda Chaudhuri*[,†]

Contribution from the Division of Lipid Science and Technology, Inorganic and Physical Chemistry Division, Indian Institute of Chemical Technology, Hyderabad-500 007, India

Received January 22, 2007; E-mail: arabinda@iict.res.in

Abstract: A number of prior studies have demonstrated that the DNA-binding and gene transfection efficacies of cationic amphiphiles crucially depend on their various structural parameters including hydrophobic chain lengths, headgroup functionalities, and the nature of the linker-functionality used in tethering the polar headgroup and hydrophobic tails. However, to date addressing the issue of linker orientation remains unexplored in liposomal gene delivery. Toward probing the influence of linker orientation in cationic lipid mediated gene delivery, we have designed and synthesized two structurally isomeric remarkably similar cationic amphiphiles **1** and **2** bearing the same hydrophobic tails and the same polar headgroups connected by the same ester linker group. The only structural difference between the cationic amphiphiles **1** and **2** is the orientation of their linker ester functionality. While lipid **1** showed high gene transfer efficacies in multiple cultured animal cells, lipid **2** was essentially transfection incompetent. Findings in both transmission electron microscopic and dynamic laser light scattering studies revealed no significant size difference between the lipoplexes of lipids **1** and **2**. Findings in confocal microscopic and fluorescence resonance energy transfer (FRET) experiments, taken together, support the notion that the remarkably higher gene transfer efficacies of lipid **1** compared to those of lipid **2** presumably originate from higher biomembrane fusogenicity of lipid **1** liposomes. Differential scanning calorimetry (DSC) and fluorescence anisotropy studies revealed a significantly higher gel-to-liquid crystalline temperature for the lipid **2** liposomes than that for lipid **1** liposomes. Findings in the dye entrapment experiment were also consistent with the higher rigidity of lipid **2**/cholesterol (1:1 mole ratio) liposomes. Thus, the higher biomembrane fusibility of lipid **1** liposomes than that of lipid **2** liposomes presumably originates from the more rigid nature of lipid **2** cationic liposomes. Taken together, the present findings demonstrate for the first time that even as minor a structural variation as linker orientation reversal in cationic amphiphiles can profoundly influence DNA-binding characteristics, membrane rigidity, membrane fusibility, cellular uptake, and consequently gene delivery efficacies of cationic liposomes.

Introduction

The clinical success of gene therapy, the modality to combat a myriad of inherited diseases, continues to remain critically dependent on the availability of safe and efficacious gene delivery reagents, popularly known as transfection vectors.[1] Broadly speaking, contemporary transfection vectors are classified into two major categories: viral and nonviral. Viral vectors, although remarkably efficient in transfecting our body cells, suffer from numerous biosafety related disadvantages. For instance, viral vectors are capable of the following: generating a potentially replication competent virus through various recombination events with the host genome; inducing inflammatory and adverse immunogenic responses; and producing insertional mutagenesis through random integration into the host genome; etc.[2] More recently, it has been reported that retrovirus vector insertion near the promoter of the proto-oncogene LMO2 in 2 human patients with X-linked severe combined immunodeficiency (SCID-XI) is capable of triggering deregulated premalignant cell proliferation with unexpected frequency.[3] In addition, viral vectors have a low insert size limit for the

[†] Division of Lipid Science and Technology.
[‡] Inorganic and Physical Chemistry Division.
[§] Present address: School of Pharmacy, University of North Carolina, Chapel Hill, NC 27599-7360, USA.
[||] Present address: Department of Chemistry and Division of Biological Engineering, Massachusetts Institute of Technology, MA 02139, USA.

(1) (a) Verma, I. M.; Somina, M. *Nature* **1997**, *389*, 239−242. (b) Anderson, W. F. *Nature* **1998**, *392*, 25−30. (c) Yla-Herttuala, S.; Martin, J. F. *Lancet* **2000**, *355*, 213−222.
(2) (a) Check, E. *Nature* **2003**, *423*, 573−574. (b) Yang, Y.; Nunes, F. A.; Berencsi, K.; Furth, E. E.; Gonczol, E.; Wilson, J. M. *Proc. Natl. Acad. Sci. U.S.A.* **1994**, *91*, 4407−4411. (c) Knowles, M. R.; Hohneker, K. W.; Zhou, Z.; Olsen, J. C.; Noah, T. L.; Hu, P. C.; Leigh, M. W.; Engelhardt, J. F.; Edwards, L. J.; Jones, K. R.; Boucher, R. A. *New Engl. J. Med.* **1995**, *333*, 823−831. (d) Crystal, R. G.; McElvaney, N. G.; Rosenfeld, M, A.; Chu, C. S.; Mastrangeli, A.; Hay, J. G.; Brody, S. L.; Jaffe, H. A.; Eissa, N. T.; Danel, C. *Nat. Genet.* **1994**, *8*, 42−51. (e) Yang, Y.; Nunes, F. A.; Berencsi, K.; Gonczol, E.; Engelhardt, J. F.; Wilson, J. *Nature.* **1994**, *401*, 517−518.
(3) Hacein-Bey-Abina, S. et al. *Science* **2003**, *401*, 415−419.

10.1021/ja0704683 CCC: $37.00

therapeutic genes they can pack inside. Consequently, an increasing number of investigations are being reported on the development of safe and efficacious nonviral alternatives including cationic amphiphiles (also known as cationic transfection lipids),[4] cationic polymers,[5] dendrimers,[6] etc. Because of their lesser immunogenic nature, robust manufacture ability to deliver large pieces of DNA, and ease of handling and preparation techniques, an upsurge of global interest has recently been witnessed in developing efficacious cationic transfection lipids for delivering genes into our body cells[7] including our own work.[8]

The molecular architectures of cationic amphiphiles consist of a positively charged water-loving (hydrophilic) polar headgroup region and a nonpolar hydrophobic tail region (usually consisting of either two long aliphatic hydrocarbon chains or a cholesterol skeleton) often tethered together via a linker functionality such as ether, ester, amide, amidine group, etc. Understanding the structural parameters capable of influencing the gene delivery efficiencies of cationic amphiphiles is essential for rational design of efficient cationic transfection lipids. To this end, the focus of many prior structure−activity investigations have been centered around probing the influence of each of these three lipid structural components in modulating the gene transfer efficacies of cationic amphiphiles. For instance, a number of prior reports have demonstrated that the gene transfer efficiencies of cationic amphiphiles critically depends on their molecular architectures including hydrophobic alkyl chain lengths,[9] nature of headgroups[8f,10] as well as on the nature of linker and spacer functionalities used in covalent tethering of the polar headgroups and the nonpolar tails of cationic amphiphiles.[8h,10,11] Recently, the in vitro gene transfer efficiency of a cationic amphiphile with asymmetric hydrocarbon chains, namely oleoyldecanoyl-ethylphosphatidylcholine (C18:1/C10-EPC), has been demonstrated to be about 50-fold superior to that of its structurally very similar saturated asymmetric counterpart stearoyldecanoyl-ethylphosphatidylcholine (C18:0/C10-EPC).[12] Toward addressing an hitherto unexplored issue in liposomal gene delivery, namely, the influence of linker orientation, in the present study, we have designed and synthesized two structurally isomeric remarkably similar cationic amphiphiles **1** and **2** (Scheme 1) bearing the same hydrophobic tails and the same polar headgroups connected by the same ester linker group. The sole structural difference between the cationic lipids **1** and **2** is the orientation of the linker functionality (ester group). Despite having such striking structural similarities, only lipid **1** could efficiently deliver plasmid DNA encoding β-galactosidase enzyme into a number of cultured mammalian cells including COS-1 (SV 40 transformed African green monkey kidney cells), CHO (Chinese hamster ovarian cells), HepG2 (Human hepatocarcinoma cells), and A549 (human lung carcinoma cells). In sharp contrast, lipid **2** was found to be essentially incompetent in delivering a β-galactosidase reporter gene into any of these cells.

The lipid/DNA complexes (lipoplexes) of both lipids **1** and **2** were found to be of similar size and morphology thereby ruling out any major role of different lipoplex sizes and shapes behind their remarkably contrasting gene delivery profiles. Findings in the confocal microscopic experiments in representative HepG2 cells using lipoplexes containing fluorescently labeled plasmid DNA revealed a significantly higher cellular uptake of lipid **1** associated DNA than that of lipid **2** associated DNA. Fluorescence resonance energy transfer (FRET) studies revealed higher membrane fusogenicity of the lipid **1**/cholesterol liposomes compared to the biomembrane fusogenicity of lipid **2**/cholesterol liposomes. Studies on the thermotropic behaviors of pure cationic liposomes of lipids **1** and **2** using techniques of differential scanning calorimetry as well as fluorescence anisotropy revealed a significantly lower gel to liquid crystalline transition temperature for the lipid **1** liposomes than that for

(4) Karmali, P. P.; Chaudhuri, A. *Med. Res. Rev.* **2007**, *27*, 696−722 and the references cited therein.

(5) (a) Mishra, S.; Heidel, J. D.; Webster, P.; Davis, M. E. *J. Control. Rel.* **2006**, *116*, 179−191. (b) Lynn, D. M.; Anderson, D. G.; Putman, D.; Langer, R. *J. Am. Chem. Soc.* **2001**, *123*, 8155−8156. (c) Choi, J. S.; Joo, D. K.; Kim, C. H.; Kim, K.; Park, J. S. *J. Am. Chem. Soc.* **2000**, *122*, 474−480.

(6) (a) Tang, M. X.; Redemann, C. T.; Szoka, F. C. *Bioconjugate Chem.* **1996**, *7*, 703−714. (b) Kukowska-Latallo, J. F.; Bielinska, A. U.; Johnson, J.; Spinder, R.; Tomalia, D. A.; Baker, J. R. *Proc. Natl. Acad. Sci. U.S.A.* **1996**, *93*, 4897−4902. (c) Luo, D.; Haverstick, K.; Belcheva, N.; Han, E.; Saltzman, W. M. *Macromolecules* **2002**, *35*, 3456−3462.

(7) (a) McGregor, C.; Perrin, C.; Monck, M.; Camilleri, P.; Anthony, Kirby, J. *J. Am. Chem. Soc.* **2001**, *123*, 6215−6220. (b) Prata, C. A.; H.; Zhao, Y.; Barthelemy, P.; Li, Y.; Luo, D.; McIntosh, T. J.; Lee, S. J.; Grinstaff, M. W. *J. Am. Chem. Soc.* **2004**, *126*, 12196−12197. (c) Bell, P. C.; Bergsma, I. P.; Bras, W.; Stuart, M. C. A.; Rowan, M. C.; Feiters, M. C.; Engberts, J. B. F. N. *J. Am. Chem. Soc.* **2003**, *125*, 1551−1558. (d) Zhu, J.; Munn, R. J.; Nantz, M. H. *J. Am. Chem. Soc.* **2000**, *122*, 2645−2646. (e) Guenin, E.; Herve, A. C.; Floch, V.; Loisel, S.; Yaounac, J. J.; Clement, J. C.; Ferec, C.; des Abbayas, H. *Angew. Chem., Int. Ed.* **2000**, *39*, 629−631. (f) Ilies, M. A.; Seitz, W. A.; Ghiviriga, I.; Johnson, B. H.; Miller, A.; Thompson, E. B.; Balaban, A. T. *J. Med. Chem.* **2004**, *15*, 3744−3754. (g) Lee, Y.; Koo, H.; Lim, Y. B.; Lee, Y.; Mo, H.; Park, J. S. *Bioorg. Med. Chem. Lett.* **2004**, *14*, 2637−2641. (h) Wang, L.; MacDonald, R. C. *Gene Ther.* **2004**, *11*, 1358−1362. (i) Kirby, A. J. et al. *Angew. Chem., Int. Ed.* **2003**, *42*, 1448−1457. (j) Ewert, K.; Ahmed, A.; Evans, H. M.; Schmidt, H. W.; Safinya, C. R. *J. Med. Chem.* **2002**, *45*, 5023−5029. (k) Floch, V.; Loisel, S.; Guenin, E.; Herve, A. C.; Clement, J. C.; Yaouanc, J. J.; des Abbayes, H.; Ferec, C. *J. Med. Chem.* **2000**, *43*, 4617−4628. (l) Oudrhiri, N.; Vigneron, J. P.; Peuchmaur, M.; Leclerc, T.; Lehn, J.-M.; Lehn, P. *Proc. Natl. Acad. Sci. U.S.A.* **1997**, *94*, 1651−1656. (m) Pitard, B.; Oudrhiri, N.; Vigneron, J. P.; Hauchecorne, M.; Aguerre, O.; Toury, R.; Airiau, M.; Ramasawmy, R.; Scherman, D.; Crouzet, J.; Lehn, J.-M.; Lehn, P. *Proc. Natl. Acad. Sci. U.S.A.* **1999**, *96*, 2621−2626. (n) Pitard, B.; Oudrhiri, N.; Lambert, O.; Vivien, E.; Masson, C.; Wetzer, B.; Hauchecorne, M.; Scherman, D.; Rigaud, J. L.; Vigneron, J. P.; Lehn, J.-M.; Lehn, P. *J. Gene Med.* **2001**, *3*, 478−487. (o) Vigneron, J. P.; Oudrhiri, N.; Fauquet, M.; Fauguet, M.; Vergely, L.; Bradley, J.-C.; Basseleville, M.; Lehn, P.; Lehn, J-M. *Proc. Natl. Acad. Sci. U.S.A.* **1996**, *93*, 9682−9986.

(8) (a) Karmali, P. P.; Majeti, B. K.; Bojja, S.; Chaudhuri, A. *Bioconjugate Chem.* **2006**, *17*, 159−171. (b) Bharat, M. K.; Karmali, P. P.; Reddy, B. S.; Chaudhuri, A. *J. Med. Chem.* **2005**, *48*, 3784−3795. (c) Sen, J.; Chaudhuri, A. *J. Med. Chem.* **2005**, *48*, 812−820. (d) Sen, J.; Chaudhuri, A. *Bioconjugate Chem.* **2005**, *16*, 903−912. (e) Mahidhar, Y. V.; Rajesh, M.; Madhavendra, S. S.; Chaudhuri, A. *J. Med. Chem.* **2004**, *47*, 5721−5728. (f) Majeti, B. K.; Singh, R. S.; Yadav, S. K.; Reddy, S. B.; Ramkrishna, S.; Diwan,P. V.; Madhavendra, S. S.; Chaudhuri, A. *Chem. Biol.* **2004**, *11*, 427−437. (g) Mahidhar, Y. V.; Rajesh, M.; Chaudhuri, A. *J. Med. Chem.* **2004**, *47*, 3938−3948. (h) Karmali, P. P.; Kumar, V. V.; Chaudhuri, A. *J. Med. Chem.* **2004**, *47*, 2123−2132. (i) Singh, R. S.; Gonçalves, C.; Sandrin, P.; Pichon, C.; Midoux, P.; Chaudhuri, A. *Chem. Biol.* **2004**, *11*, 713−723. (j) Kumar, V. V.; Pichon, C.; Refregiers, M.; Guerin, B.; Midoux, P.; Chaudhuri, A. *Gene Ther.* **2003**, *10*, 1206−1215.

(9) (a) Heyes, J. A.; Duvaz, D. N.; Cooper, R. G.; Springer, C. J. *J. Med. Chem.* **2002**, *45*, 99−114. (b) Fichert, T.; Regelin, A.; Massing, U. *Bioorg. Med. Chem. Lett.* **2000**, *10*, 787−791. (c) Byk, G.; Dubertret, C.; Escriou, V.; Frederic, M.; Jaslin, G.; Rangara, R.; Pitard, B.; Crouzet, J.; Wils, P.; Schwartz, B.; Scherman, D. *J. Med. Chem.* **1998**, *41*, 224−235. (d) Felgner, J. H.; Kumar, R.; Sridhar, C. N.; Wheeler, C. J.; Tsai, Y. J.; Border, R.; Ramsey, P.; Martin, M.; Felgner, P, L. *J. Biol. Chem.* **1994**, *269*, 2550−2561. (e) Singh, R. S.; Mukherjee, K.; Banerjee, R.; Chaudhuri, A.; Hait, S. K.; Moulik, S.; Ramadas, Y.; Vijayalakshmi, A.; Rao, N. M. *Chem.−Eur. J.* **2002**, *8*, 900−909. (f) Srilakshmi, G. V.; Sen, J.; Chaudhuri, A.; Ramdas, Y.; Rao, N. M. *Biochim. Biophys. Acta (Biomembranes)* **2002**, *1559*, 87−95.

(10) (a) Banerjee, R.; Mahidhar, Y. V.; Chaudhuri, A.; Gopal, V.; Rao, N. M. *J. Med. Chem.* **2001**, *44*, 4176−4185. (b) Banerjee, R.; Das, P. K.; Srilakshmi, G. V.; Chaudhuri, A.; Rao, N. M. *J. Med. Chem.* **1999**, *42*, 4292−4299.

(11) (a) Ghosh, Y. K.; Visweswariah, S. S.; Bhattacharya, S. *FEBS Lett.* **2000**, *473*, 341−344. (b) Singh, R. S.; Chaudhuri, A. *FEBS Lett.* **2004**, *556*, 86−90. (c) Ghosh, Y. K.; Viswesaraiah, S. S.; Bhattacharya, S. *Bioconjugate Chem.* **2002**, *13*, 378−384.

(12) Koynova, R.; Wang, Li.; MacDonald, R. C. *Proc. Natl. Acad. Sci. U.S.A.* **2006**, *103*, 14373−14378.

Scheme 1[a]

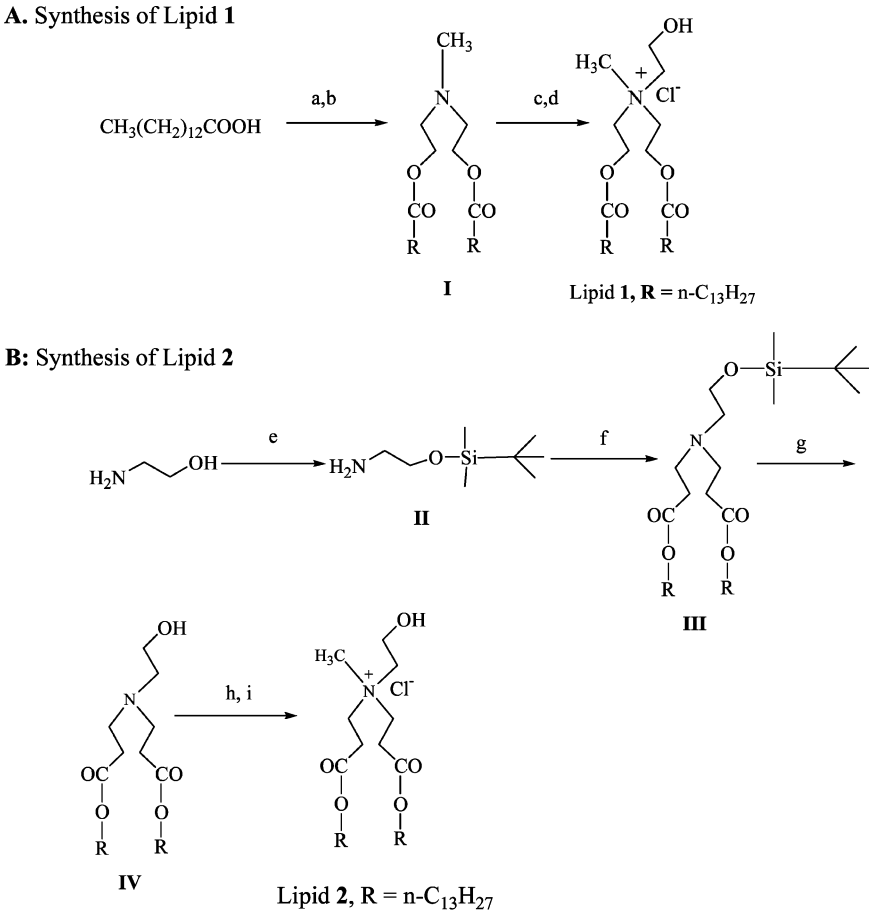

[a] Reagents: (a) $SOCl_2$ (1.5 equiv), pyridine (1.5 equiv), 0 °C−rt, DCM, 2 h; (b) *N*-methyl-*N*,*N*-diethanol amine (0.4 equiv), DMF, 0 °C−rt, 4 h, 1 N aq NaOH/DCM (biphasic system); (c) 2-bromoethanol (1.5 equiv), 85 °C, 4 h; (d) Amberlyst A-26 chloride ion exchange resin; (e) TBDMS-Cl (1.5 equiv), Imidazole (1.5 equiv), dry DCM 0 °C−rt, 12 h; (f) $CH_3(CH_2)_{10}CH_2CH_2OCOBr$ (2.5 equiv), K_2CO_3 (3 equiv), ethylacetate, reflux, 48 h; (g) TBAF (1.5 equiv), dry THF, 6 h; (h) MeI, DCM, 12 h; (i) Amberlyst A-26 chloride ion exchange; (j) $SOCl_2$ (1.5 equiv), pyridine (1.5 equiv), $CH_3(CH_2)_{11}CH_2OH$ (1.2 equiv), DCM, 0 °C−rt, 2 h.

lipid **2** liposomes. Findings in the dye entrapment experiment were also consistent with the higher rigidity of lipid **2**/cholesterol (1:1 mole ratio) liposomes. Thus, the higher biomembrane fusibility of lipid **1** liposomes than that of lipid **2** liposomes presumably originates from the more rigid nature of lipid **2** cationic liposomes. Taken together, the present findings demonstrate for the first time that even as minor a structural variation as linker orientation reversal in cationic amphiphiles can profoundly influence DNA-binding characteristics, membrane rigidity, membrane fusibility, cellular uptake, and consequently gene delivery efficacies of cationic liposomes.

Results

Chemistry. Toward probing the influence of the structural orientation of the linker functionality, we designed lipids **1** and **2** (Scheme 1) such that the two lipids architecturally differ only in the orientation of their head−tail linker functionality (ester group). Lipid **1** was synthesized by coupling myristic acid with *N*-methyl-*N*,*N*-diethanolamine followed by quaternization with 2-bromoethanol and chloride ion exchange chromatography over Amberlyst-A26 resin (Scheme 1A). Lipid **2** was prepared by di-N-alkylation of *O*-*tert*-butyl-dimethylsilyl-2-aminoethanol with *n*-tridecyl-3-bromopropanoate ester, followed by TBDMS-deprotection with tetrabutylammonium fluoride, quaterization with methyl iodide, and chloride ion-exchange chromatography over Amberlyst A-26 (Scheme 1B). The *n*-tridecyl-3-bromopropanoate ester was synthesized by reacting 3-bromopropanoic acid with thionyl chloride followed by esterification of the resulting acid chloride with *n*-tridecyl alcohol (step j, Scheme 1C). The structures of all the intermediates (Scheme 1) were confirmed by ^{1}H NMR spectral analysis, and the structures of the final target lipids **1** and **2** were confirmed by both NMR and mass spectral analysis. The purities of the final lipids were confirmed by both elemental (C, H, N, Cl) and analytical HPLC analysis in two different mobile phases. ^{1}H NMR spectra of all the intermediates **I**−**V** (Scheme 1), ^{1}H NMR and mass spectra of the final lipids **1** and **2**, and the HPLC chromatograms for

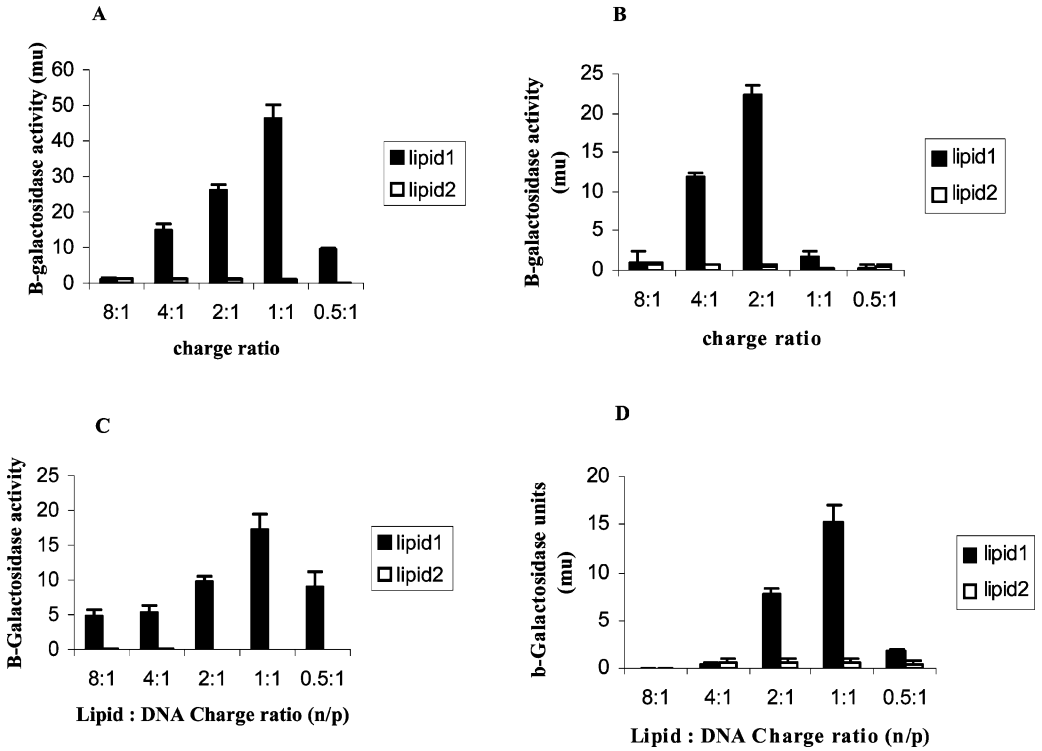

Figure 1. In vitro gene delivery efficiencies of lipids **1** and **2** into COS-1 (A), CHO (B), HepG-2 (C), and A-549 (D) cells using cholesterol as co-lipid (at a lipid/cholesterol mole ratio of 1:1). Units of β-galactosidase activity were plotted against the varying lipid-to-DNA ($\pm$) charge ratios. Transfection experiments were performed as described in the text. The transfection values shown are the average of triplicate experiments performed on the same day.

the final lipids **1** and **2** in two different mobile phases (100% methanol and 95:5 methanol/water, v/v) are available in Figures S1−S11 of the Supporting Information.

Transfection Biology. A reporter gene expression assay was used in evaluating the in vitro gene delivery efficacies of lipids **1** and **2** in four cultured mammalian cells including COS-1 (SV 40 transformed African green monkey kidney cells), CHO (Chinese hamster ovary cells), HepG2 (human hepatocarcinoma), and A549 (human lung carcinoma cells) using p-CMV-SPORT-β-gal plasmid DNA as the reporter gene encoding the enzyme β-galactosidase across the lipid/DNA charge ratio ($\pm$) range 8:1−0.5:1. Despite the opposite orientation of the linker ester functionality being the only structural differences between lipids **1** and **2**, only lipid **1** was competent in delivering genes into these four cells (Figure 1A−D). Lipid **1** showed its optimal gene delivery efficacies at a lipid/DNA charge ratio of 1:1 in COS-1, HepG2, and A549 cells (Figure 1A, C, and D, respectively, filled bars) and at lipid/DNA charge ratios of 2:1 in CHO cells (Figure 1B, filled bars). In sharp contrast, lipid **2** turned out to be essentially incompetent in delivering genes into any of these four cells across the entire lipid/DNA charge ratios of 8:1−0.5:1 (Figure 1A−D, open bars). Equimolar amounts of cholesterol (with respect to cationic lipids) were used as the co-lipid (DOPE, the other commonly used co-lipid in liposomal gene delivery, failed to impart gene transfer properties to both lipids **1** and **2**; data not shown). Thus, the relative transfection profiles of lipids **1** and **2** summarized in Figure 1A−D demonstrate that the orientation of the linker functionality used in tethering the nonpolar tails and polar heads of cationic amphiphiles is a crucial structural parameter in liposomal gene delivery.

Physicochemical Characterizations of Liposomes and Lipoplexes. Sizes and Zeta Potentials. The sizes and surface potentials of the lipid **1** and lipid **2** lipoplexes (prepared in DMEM) were measured using a dynamic laser light scattering technique (Zetasizer 3000A, Malvern Instruments, U.K.). The sizes of both lipids **1** and **2** lipoplexes were found to be similar for lipoplexes having the same lipid/DNA charge ratios, and interestingly, the sizes of both the lipoplexes steadily increased from 200 to 600 nm as the lipid/DNA charge ratios increased from 0.5:1 to 8:1(Table 1A).

Findings in the transmission electron microscopic (TEM) studies also revealed no significant size and morphological differences between the liposomes and lipoplexes prepared with lipids **1** and **2** (representative TEM pictures for lipoplexes prepared using lipid/DNA charge ratios of 1:1 are shown in Figure S12, Parts A−D, Supporting Information). Interestingly, while the net surface potentials of lipid **1** lipoplexes remained positive for the lipid/DNA charge ratios higher than 1:1, those for lipid **2** lipoplexes remained negative across the entire lipid/DNA charge ratio range 0.5:1−4:1 (Table 1B).

Lipid/DNA Binding Interactions and DNase I Sensitivities. The electrostatic binding interactions between the plasmid DNA and lipids **1** and **2** at varying lipid/DNA charge ratios were measured by the conventional gel retardation assay. The electrophoretic gel patterns revealed an interesting feature. While both the lipids were capable of completely inhibiting the electrophoretic mobility of plasmid DNA when lipoplexes were prepared at a high lipid:DNA charge ratio of 8:1, significant free DNA bands were found in both the lipoplexes at the lower lipid/DNA charge ratios of 0.5:1 and 1:1 (Figure 2A). DNase I sensitivity assays were carried out across the lipid/DNA charge

Table 1. (A) Hydrodynamic Diameters of the Lipoplexes Across the Lipid/DNA Charge Ratios 0.5:1−8:1[a] and (B) Zeta Potentials (ξ, mV) of Lipoplexes

A. hydrodynamic diameters

lipid		lipid/DNA (±) (0.5:1)	lipid/DNA (±) (1:1)	lipid/DNA (±) (2:1)	lipid/DNA (±) (4:1)	lipid/DNA (±) (8:1)
lipid **1**	size (nm)	(210 ± 8)	(216 ± 2)	(350 ± 13)	(537 ± 17.)	(615 ± 65)
lipid **2**	size (nm)	(214 ± 18)	(227 ± 9)	(346 ± 19)	(445 ± 36)	(579 ± 21)

B. zeta potentials

	lipid/DNA (±) (0.5:1)	lipid/DNA (±) (1:1)	lipid:DNA (±) 2:1	lipid/DNA (±) (4:1)	lipid/DNA (±) (8:1)
lipid **1**	−8 ± 1	−1.8 ± 0.8	13.2 ± 2.7	15.8 ± 1.8	21.6 ± 2.8
lipid **2**	−29.2 ± 4.2	−24.2 ± 2.2	−20.9 ± 2.2	−2.2 ± 2.5	5.6 ± 1.7

[a] The sizes and the surface potentials of the lipoplexes prepared in the presence of plain DMEM were measured by the laser light scattering technique using Zetasizer 3000A (Malvern Instruments, U.K.) as described in the text. Values shown are the averages obtained from three (sizes) and ten (zeta potentials) measurements.

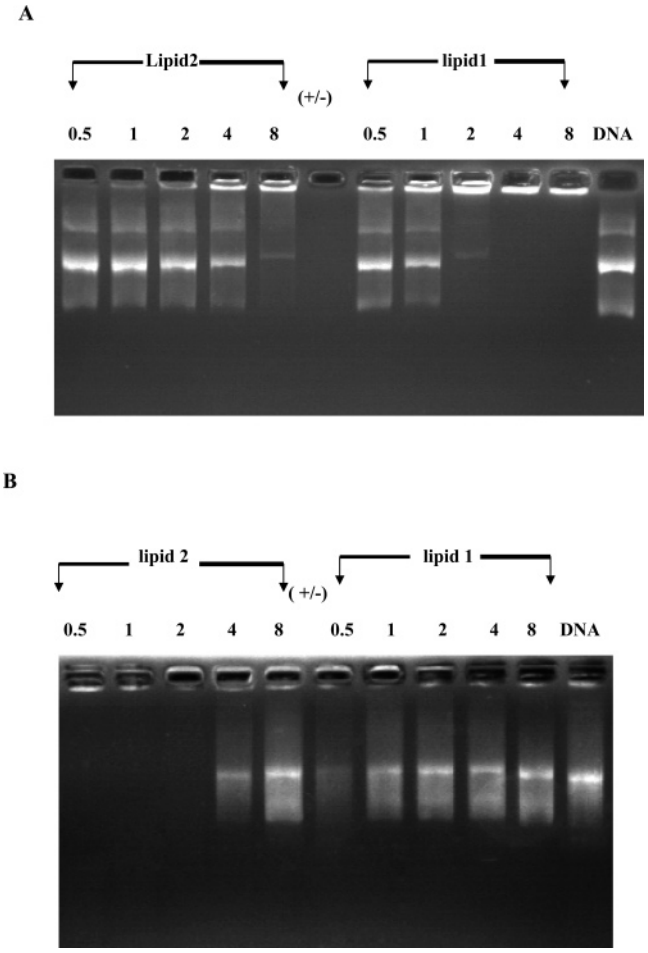

Figure 2. Electrophoretic gel patterns for lipoplex-associated DNA in gel retardation assay (A) and in DNase I sensitivity assay (B). The lipid/DNA charge ratios are indicated at the top of each lane. The details of the treatment are as described in the text.

ratios 0.5:1−8:1. After the free DNA digestion by DNase I, the total DNA (both digested and inaccessible DNA) was separated from the lipids and DNase I (by extracting with organic solvent) and loaded onto a 1% agarose gel. The band intensities of inaccessible and therefore undigested DNA associated with transfection incompetent lipid **2** were found to be significantly less compared to those associated with transfection efficient lipid **1** across the lipid/DNA charge ratios 4:1−0.5:1 (Figure 2B).

Cell Viabilities. MTT-based cell viability assays were performed in representative CHO cells using lipoplexes of both lipids **1** and **2** across the entire range of lipid/DNA charge ratios used in the actual transfection experiments (8:1−0.5:1). Percent cell viabilities were found to be significantly high across the entire lipid/DNA charge ratios when cells were treated with lipoplexes prepared with either lipid **1** or **2** (more than 80%, data shown in Figure S13, Supporting Information).

Cellular Uptake Studies. The relative cellular uptake of plasmid DNA were measured in representative HepG2 cells by incubating lipoplexes (containing lipid/DNA charged ratio of 1:1 where lipid **1** showed its optimal transfection efficiency in HepG2 cells) prepared with lipids **1** and **2** and a fluorescein-labeled p-CMV-SPORT-β-Gal for 4 h at 37 °C. After washing the cells with phosphate buffer saline, live HepG2 cells were viewed with a confocal microscope. Although a number of fluorescein-labeled cells were visible when the cells were treated with lipid **1** lipoplex (Figure 3A−C), hardly any fluorescein-labeled cells could be detected when cells were treated with the lipoplex of lipid **2** (Figure 3D−F). Similarly, relative cellular uptake of the Rho-PE labeled lipoplexes of lipids **1** and **2** were studied in HepG2 cells. A number of HepG2 cells were found to be labeled red when cells were incubated with Rho-PE labeled lipid **1** lipoplexes for 4 h while hardly any HepG2 cells were found to be labeled red upon the same treatment with Rho-PE labeled lipid **2** lipoplexes (epifluorescence microscopic images for cellular uptake experiments using Rho-PE labeled lipoplexes are shown in Figure S14, Supporting Information).

Membrane Fusogenicities of Liposomes. Relative biomembrane fusogenicities of the liposomes prepared from lipids **1** and **2** (using equimolar amounts of cholesterol as co-lipid) were assessed by using a fluorescence resonance energy transfer (FRET) assay. Because of spatial proximity, fluorescence energy transfer ensues from *N*-(7-nitro-2-oxa-1,3-diazol-4-yl)-1,2-dihexadecanoyl-*sn*-glycero-3-phosphoethanolamine (NBD-PE) (energy donor) to RhodamineRed-*x*-1,2-dihexadecanoyl-*sn*-glycero 3-phosphoethanolamine (Rho-PE) (energy acceptor) when the biomembrane mimicking liposomal formulations (dioleyol-phosphatidylcholine/dioleyol-phosphatidylethanolamine/dioleyol-phosphatidylserine/cholesterol (DOPC/DOPE/DOPS/Chol) at 45:20:20:15, w/w) containing these two fluorophores are excited at the excitation wavelength of NBD-PE (485 nm). Emission at 595 nm (emission wavelength of Rho-PE) was measured.

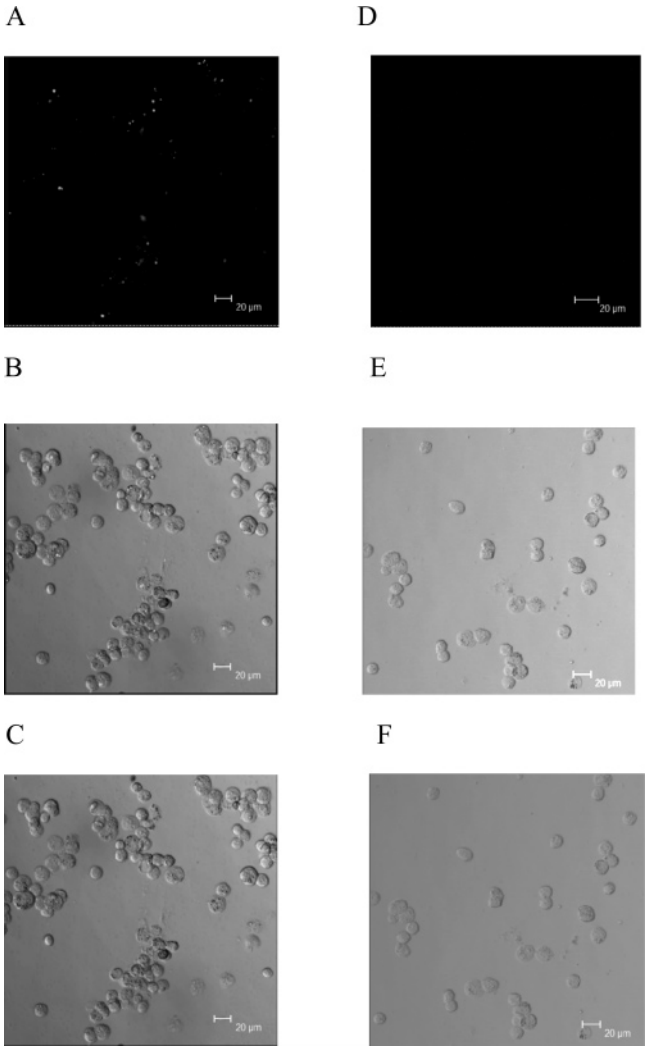

Figure 3. Confocal microscopic images of HepG2 cells transfected with lipoplexes of lipid **1** (A−C) and lipoplexes of lipid **2** (D−F) containing fluorescein-labeled plasmid DNA. Lipid/DNA charge ratios in both the lipoplexes were maintained at 1:1. (A and D) Fluoroscent images. (B and E) Overlay images. (C and F) Phase contrast bright field images. The details of confocal microscopic experiments are as described in the text.

Fluorescence intensities of the double fluorophore labeled biomembrane mimicking liposomes were also measured in the presence of 1% Triton X-100 after ensuring complete mixing of the lipids, and these intensities were used for normalization (to 100% fusions) of measurements. The results summarized in Figure 4 clearly demonstrate that the cationic liposomes of lipid **1** possess about a 3.5-fold higher biomembrane fusogenicity than that of the liposomes of lipid **2**. These relative biomembrane fusogenicity profiles for the cationic liposomes of lipids **1** and **2** did not change significantly when an FRET experiment was conducted monitoring the increase in the emission intensity NBD-PE (% normalized fluorescence recovery vs time plot obtained by measurements of increasing emission intensities of NBD-PE are shown in Figure S15, Supporting Information).

Thermotropic Phase Behaviors of Lipid 1 and Lipid 2 Liposomes by Differential Scanning Calorimetry and Fluorescence Anisotropy. The thermograms obtained for the pure cationic liposomes of lipids **1** and **2** (Figure 5A) in a differential scanning calorimetric (DSC) study revealed a significantly higher gel to liquid crystalline transition temperature (T_m) for lipid **2** liposomes (49 °C) than that for lipid **1** liposomes

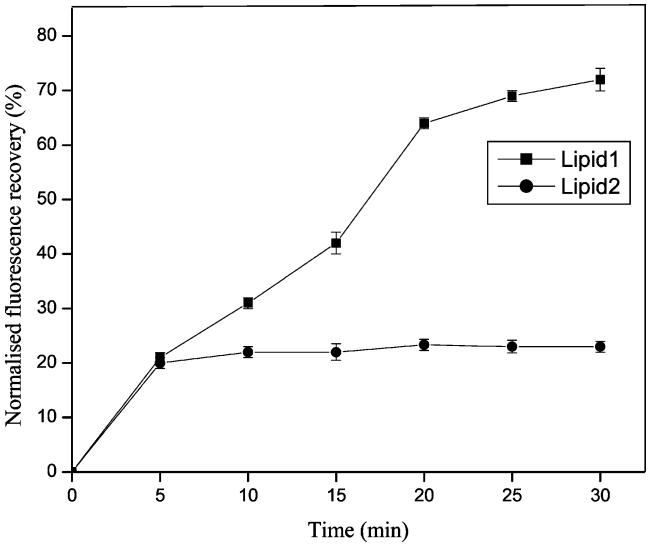

Figure 4. Biomembrane fusogenicities of lipid **1**/Chol and lipid **2**/Chol liposomes. Fusion was induced by adding the cationic lipid **1**/Chol and lipid **2**/Chol liposomes to the double fluorophore labeled biomembrane mimicking DOPC/DOPE/DOPS/Chol liposomal formulations. The values shown are representative of three independent measurements. The details of FRET experiments are as discussed in text.

(34 °C). The gel to liquid crystalline temperatures of the lipid **1** and lipid **2** liposomes were also studied by the technique of fluorescence anisotropy using 1,6-diphenyl-1,3,5-hexatriene (DPH) as the fluorescence probe. Consistent with the findings in the DSC study (Figure 5A), the midpoint of transition (the transition temperature) for the lipid **1** liposomes was found to be close to 34 °C in the fluorescence anisotropy study (Figure 5B). However, no sharp midpoint transition temperature was detected in the fluorescence anisotropy study for lipid **2** liposomes (Figure 5B).

Dye Entrapment Experiments. Finally, toward probing the inherent membrane rigidity differences, if any, between the cationic liposomes of lipids **1** and **2** containing equimolar amounts of cholesterol (liposomes used in the actual transfection experiments), a simple dye entrapment experiment was carried out using cholesterol containing liposomes with entrapped 5/6-carboxyfluorescein (CF), a fluorescent dye soluble in 10 mM Tris·HCl buffer at pH 8. The relative amount of CF released (i.e., % permeation of CF) in 60 min from the lipid **2**/cholesterol liposome was found to be significantly less than that released from the lipid **1**/cholesterol liposomes (data shown in Figure S16, Supporting Information). Such a remarkably decreased release of entrapped CF from lipid **2**/cholesterol liposomes strongly supports the notion that the membrane rigidity of lipid **2**/cholesterol (1:1 mole ratio) liposomes is significantly higher than that of lipid **1**/cholesterol (1:1 mole ratio) liposomes.

Discussion

Systematic structure−activity investigations aimed at understanding how variations in the lipid structural components including polar headgroups, nonpolar hydrocarbon tails, and the linker functionalities influence the gene transfer efficacies of cationic amphiphiles continue to remain an actively pursued area of research in nonviral gene delivery.[8f,g,9a−f,10,11,13] The nature

(13) Niculescu-Duvaz, D.; Heyes, J.; Springer, C. J. *Curr. Med. Chem.* **2003**, *10*, 1233−1261.

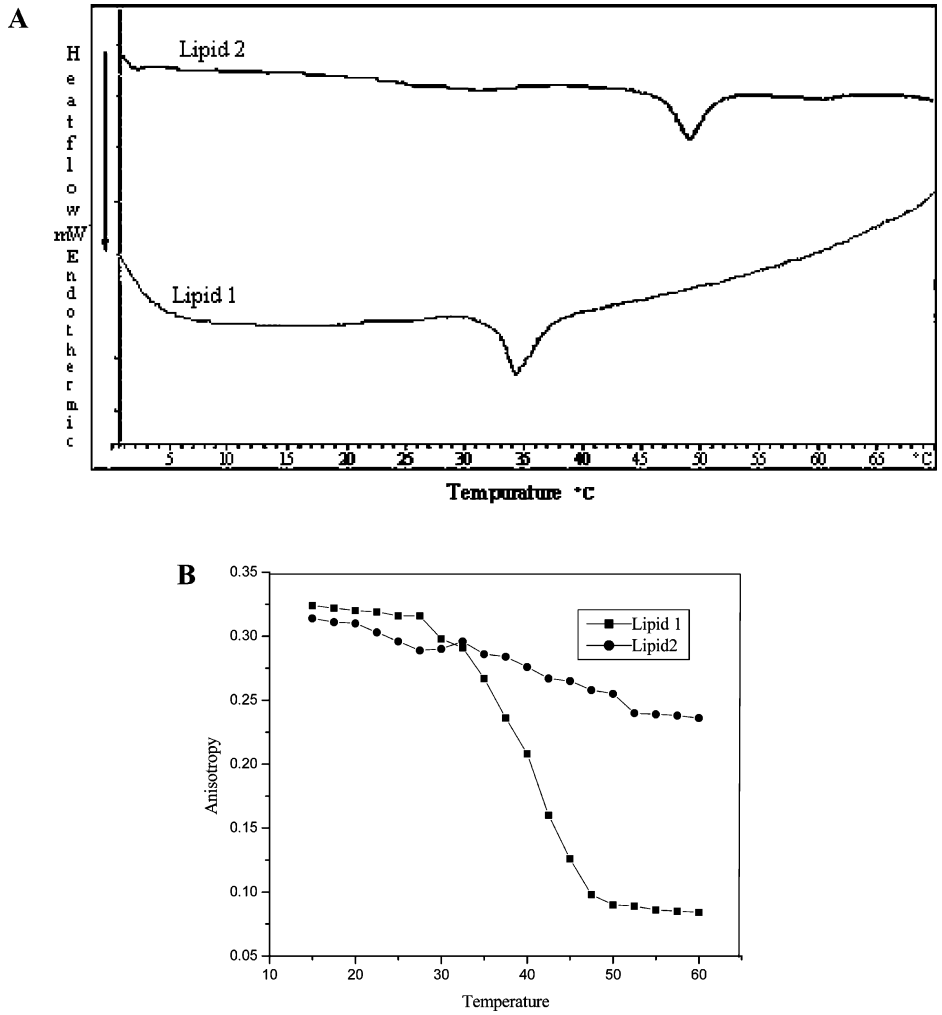

Figure 5. DSC thermograms of cationic liposomes of lipids **1** and **2** (A); fluorescence anisotropy vs temperature plots for lipid **1** and lipid **2** liposomes (B). Details of experiments are as described in text.

of the linker group in particular plays a dominant role in modulating gene delivery efficiencies of cationic lipids. The relative orientation of the cationic headgroup and hydrocarbon anchor is governed by the nature of the linker bond bridging them. The linker group controls the conformational flexibility, degree of stability, biodegradibility, and, hence, the gene transfer efficacy of a cationic amphiphile. Most commonly used linker groups include ethers, esters, carbamates, amides, carbonates, phosphonates, disulfides, etc. A number of prior reports demonstrated advantages of one class of linker functionality over the others. For instance, cholesterol-based cationic amphiphiles with an ether linker functionality have been demonstrated to exhibit superior in vitro gene transfer efficacies to their ester counterparts.[11a,c] Ester and carbonate linkers are biodegradable and less toxic but not stable chemically.[14] The phosphate diester bond (as in DOPE) is biodegradable and has a chemical stability higher than that of esters but lower than that of amides. On the other hand, phosphonates are hydrolytically more stable than phosphates and presumably more biodegradable.[15] The length of the linker determines the level of hydration of a lipid. Incorporating oxyethylene units between the cholesterol moiety and the headgroup has been reported to increase the level of hydration and decrease the transfection activity.[11c] However, to date addressing the issue of linker orientation remains unexplored in liposomal gene delivery. To this end, we have designed in the present investigation two structurally very similar cationic amphiphiles **1** and **2** (Scheme 1) differing only in the orientation of their ester linker functionality. As demonstrated by the transfection results described above, despite having such close structural resemblances, the gene transfer efficiencies of lipid **1** were found to be strikingly superior to those of the essentially transfection incompetent lipid **2** in multiple cultured cells.

In order to gain insights into the possible origin of such contrasting transfection profiles of the two structurally seemingly close cationic lipids **1** and **2**, first we studied the size and morphological characteristics of the lipoplexes of both lipids **1** and **2** using techniques of transmission electron microscopy (TEM) and dynamic light scattering (DLS). Measurements of the hydrodynamic diameters of both the lipoplexes (prepared across the varying lipid/DNA charge ratios of 0.5:1−8:1) by the dynamic light scattering technique revealed no significant differences in lipoplex sizes. The sizes of both the lipoplexes prepared with lipids **1** and **2** were found to similarly increase with increasing lipid/DNA charge ratios from around 200 nm

(14) Aberle, A. M.; Tablin, F.; Zhu, J.; Walker, N. J.; Gruenert, D. C.; Nantz, M. H. *Biochemistry* **1998**, *37*, 6533−6540.
(15) Duvaz-N. D.; Heyes, J.; Springer, C. J. *Curr. Med. Chem.* **2003**, *10*, 1233−1261.

at the lipid/DNA charge ratio 0.5:1 to around 600 nm at the lipid/DNA charge ratio 8:1 (Table 1A). Consistent with these findings, transmission electron microscopic studies of representative liposomes and lipoplexes (prepared with lipid/DNA charge ratios of 1:1) of both lipids **1** and **2** revealed no significant difference in their size and morphological characteristics (transmission electron micrographs of these representative liposomes and lipoplexes are shown in Figure S12, Parts A−D, Supporting Information). These findings ruled out the possibility of lipoplex sizes playing any dominant role behind the contrasting gene transfer properties of lipids **1** and **2**.

Lipid **1** lipoplexes were transfection efficient mostly at a lipid/DNA charge ratio of 1:1 (Figure 1). Both gel retardation (Figure 2A) and DNase I sensitivity (Figure 2B) assays showed the presence of a significant amount of free DNA in the lipid **1** lipoplex containing this lipid:DNA charge ratio of 1:1. Thus, full association of lipid **1** to DNA and full protection from degredation by DNase I appear to be irrelevant to the transfection activity of lipid **1**. The surface potential of lipid **1** lipoplex at the optimal lipid/DNA charge ratio 1:1 was found to be slightly negative (-1.8 ± 0.8 mV, Table 1B). The electrophoretic gel patterns in the gel retardation assay and DNase I sensitivity assay for the lipid **2** lipoplexes as well as the surface potential of the lipid **2** lipoplex at a lipid/DNA charge ratio of 4:1 (-2.2 ± 2.5 mV, Table 1B) were comparable to those for lipid **1** lipoplexes at its optimal lipid/DNA charge ratio of 1:1 (Figure 2A−B and Table 1B). Putting it differently, if lipid/DNA binding interactions and lipoplex surface potentials are key transfection modulating physicochemical parameters for the present class of cationic amphiphiles, lipid **2** should have shown comparable levels of transfection activity to those of lipid **1** at the lipid/DNA charge ratio 4:1. However, as summarized in the transfection results depicted in Figure 1, lipid **2** maintained its transfection incompetent nature at the 4:1 lipid/DNA charge ratio. Thus, the transfection results (Figure 1), lipoplex surface potential characteristics (Table 1B), lipid/DNA binding interactions (Figure 2A), and DNase I sensitivities of lipid associated DNA (Figure 2B), taken together, are consistent with the notion that some other physicochemical property (i.e., other than lipoplex surface potentials, lipid/DNA binding interactions, and the DNase I sensitivity of the lipid associated DNA) is likely to play a dominant role behind the contrastingly different transfection properties of lipids **1** and **2**. Since more than 80% CHO cells remained viable upon treatment with lipids **1** and **2** lipoplexes across the entire lipid/DNA charge ratios 8:1−0.5:1 (Figure S13, Supporting Information), varying cellular toxicities were also ruled out as a possible factor behind the contrasting transfection profiles of lipids **1** and **2**.

Toward probing the influence of relative DNA uptake profiles in modulating the transfection properties of the lipid **1** and lipid **2** lipoplexes, representative HepG2 cells were treated with both lipid **1** and lipid **2** lipoplexes prepared with a fluorescein-labeled pCMV-SPORT-β-gal plasmid DNA and cellular uptake of fluorescently labeled plasmid DNA was monitored by confocal microscopy. The findings in the confocal microscopic studies (Figure 3A−F) clearly demonstrated that the essentially transfection incompetent nature of lipid **2** is likely to originate from the extremely poor cellular uptake of plasmid DNA associated with lipid **2**. In order to gain insights into whether such contrastingly enhanced DNA uptake profiles of the lipid **1** and lipid **2** lipoplexes (Figure 3A−F) could possibly be related to any inherent biomembrane fusogenicity differences between lipids **1** and **2** liposomes, we next evaluated the relative membrane fusogenicities of both the lipid **1** and lipid **2** liposomes with a popular biomembrane mimicking liposomal formulation (dioleyol-phosphatidylcholine/dioleyol-phosphatidylethanolamine/dioleyol-phosphatidylserine/cholesterol at 45:20:20:15, w/w) by using fluorescence resonance energy transfer (FRET) technique pioneered by Struck et al.[16] This technique depends upon the interactions that occur between two fluorophores when the emission band of one (the energy donor) overlaps with the exicitation band of the second (the energy acceptor) and when such fluorophores are in close physical proximity. These conditions are satisfied when the biomembrane mimicking liposomal formulations are prepared with both the donor and the acceptor fluorophores such as *N*-(7-nitro-2-oxa-1,3-diazol-4-yl)-1,2-dihexadecanoyl-*sn*-glycero-3-phosphoethanolamine (NBD-PE) and Rhodamine Red-x-1,2-dihexadecanoyl-*sn*-glycero 3-phosphoethanolamine (Rho-PE), respectively. In such liposomes, the energy from a photon absorbed by the energy donor, NBD-PE, is transferred to the energy acceptor, Rho-PE, causing the latter to fluoresce as if it is excited directly. Since the efficiency of the FRET between two such fluorophores critically depends upon their spatial separation, any fusion event of such double-fluorophore containing biomembrane mimicking liposomes with cationic liposomes of lipids **1** and **2** (devoid of any fluorophore) decreases the efficiency of resonance energy transfer. In other words, the decrease in percent of normalized fluorescence recovery (i.e., maximum fusion corresponding to Rho-PE fluorescence emission intensity at 595 nm observed when the double-fluorophore labeled biomembrane liposomal formulation is completely disrupted with 1% Triton X-100) provides evidence for reduced membrane fusion.

The percent of normalized fluorescence recovery was found to be about 3.5-fold higher when the double-fluorophore labeled biomembrane mimicking liposomal formulations was incubated with lipid **1**/cholesterol liposomes for 30 min compared to the normalized fluorescence recovery (%) upon treatment of the biomembrane mimicking liposomes with lipid **2**/cholesterol liposomes for the same time period (Figure 4). Such FRET results are consistent with significantly higher biomembrane fusogenicities for lipid **1**/cholesterol liposomes than those for lipid **2**/cholesterol liposomes. The remarkably higher biomembrane fusogenicity for lipid **1**/cholesterol liposomes than those for lipid **2**/cholesterol liposomes (Figure 4) was fully consistent with the findings in the cellular uptake study using with Rho-PE labeled lipoplexes of lipids **1** and **2** in representative HepG2 cells. A number of Rho-PE labeled HepG2 cells were detected in the inverted epifluorescence microscopic study when cells were incubated with Rho-PE labeled lipid **1** lipoplexes while hardly any Rho-PE cell could be seen upon similar treatment of the cells with Rho-PE labeled lipoplexes of lipid **2** (the epifluorescence fluorescence micrographs for cellular uptake studies using Rho-PE labeled lipoplexes in HepG2 cells are shown in Figure S14 of the Supporting Information). Thus, the poor biomembrane fusibility of lipid **2** liposomes is likely to play a major role in the severely compromised transfection efficacies of lipid **2**. Currently believed intracellular pathways

(16) Struck, D. K.; Hoekstra, D.; Pagano, R. E. *Biochemistry* **1981**, *20*, 4093−4099.

involved in cationic lipid mediated gene transfer (lipofection) include the following: (a) endocytotic cellular uptake of the lipid/DNA complex (lipoplex); (b) release of DNA from the resulting endosomes into the cell cytoplasm; and (c) the nuclear transport of the endosomally released DNA followed by transcription and gene expression.[17−20] Improved biomembrane fusogenicity of cationic liposomes is expected to mediate not only the enhanced cellular uptake of the cationic liposome associated DNA (step a) but also the efficacy of step b. This is because efficient release of DNA from endosomes into cell cytoplasm (step b) is likely to depend on how efficiently the cationic lipids can fuse with the anionic lipid components of the endosomal membranes. Thus, enhanced biomembrane fusogenicity of cationic liposomes are likely to correlate with the transfection efficiency of cationic lipids as found in the present study. Wang and MacDonald have also found a similar correlation between membrane fusogenicity and transfection efficacies of cationic liposomes.[21]

In order to understand whether the origin of the contrasting biomembrane fusibility of lipid **1**/cholesterol and lipid **2**/cholesterol liposomes (Figure 4) could possibly be related to the differences in the inherent membrane fluidity differences of the cationic liposomes of lipids **1** and **2**, next we studied the thermotropic behaviors of the pure cationic liposomes of lipids **1** and **2** by both differential scanning calorimetry (DSC) and fluorescence anisotropy. DSC thermograms (Figure 5A) revealed the existence of a significantly higher solid gel to fluid liquid crystalline-like phase transition temperature (T_m, a property typical of membranous liposomal aggregates) for lipid **2** liposomes (49 °C) compared to that for lipid **1** liposomes (34 °C). This finding (Figure 5A) is consistent with a higher inherent membrane rigidity of the lipid **2** liposomes (compared to that of lipid **1** liposomes). The results in the fluorescene anisotropy studies further confirmed the higher membrane rigidity of lipid **2** liposomes. The fluorescence anisotropy values (r) increase with increasing membrane rigidity of the liposomal aggregates, and T_m values of liposomal aggregates are determined from the midpoints of the sigmoidal r vs temperature plots. Consistent with the findings in the DSC study (Figure 5A), lipid **1** liposomes showed a clear midpoint transition temperature (T_m) close to 34 °C in the fluorescence anisotropy study (Figure 5B). However, the fluorescence anisotropy values remained high (0.32−0.25) throughout the entire temperature range (15−60 °C) thereby demonstrating a significantly higher rigidity of the lipid **2** liposomes compared to lipid **1** liposomes (Figure 5B). Interestingly, neither the DSC nor the fluorescence anisotropy study revealed the existence of any clear gel to liquid crystalline temperature or midpoint transition temperatures when lipid **1** and lipid **2** liposomes containing equimolar amounts of cholesterol (with respect to cationic lipids) were used instead of using pure cationic liposomes (data not shown). Such absences of any pronounced reduction in fluorescence anisotropy values for the equimolar cholesterol containing liposomes of lipids **1** and **2** across the entire temperature range of 15−60 °C are consistent with the remarkable rigid nature of these equimolar cholesterol containing cationic liposomes.

As discussed above, the findings in the DSC and fluorescence anisotropy studies provided enough evidence for the existence of higher membrane rigidity in pure cationic liposomes of lipid **2** compared to that for pure cationic liposomes of lipid **1**. However, the findings in these thermotropic studies were not insightful enough to probe any inherent membrane rigidity differences between the transfection efficient lipid **1**/cholesterol (1:1 mole ratio) liposomes and transfection incompetent lipid **2**/cholesterol (1:1 mole ratio) liposomes. To this end, toward qualitative probing of the differences in the membrane rigidity of the equimolar cholesterol containing liposomes of lipids **1** and **2** (used in the actual transfection experiments), finally we carried out a simple fluorescent dye entrapment experiment. A significantly higher amount of fluorescent dye (CF) released from lipid **1**/cholesterol (1:1 mole ratio) in 60 min compared to the amount of CF released from the lipid **2**/cholesterol (1:1) liposomes during the same time interval (Figure S16, Supporting Information) provided strong evidence for the existence of higher membrane rigidity in lipid **2**/cholesterol. Use of cationic liposomes with less rigid or more fluid membranes are known to be an advantage in transfection.[9e,22−24] Cationic liposomes with fluid membranes are likely to fuse more efficaciously with both cellular plasma membranes and endosomal membranes. Thus, the significantly greater membrane fluidity of the lipid **1**/cholesterol liposomes than that of lipid **2**/cholesterol liposomes is likely to play a dominant role in the strikingly superior transfection efficacies of lipid **1**/cholesterol liposomes. The higher membrane rigidity of the lipid **2**/cholesterol liposomes presumably originate from enhanced headgroup hydration. Hydration of ester carbonyl groups (through hydrogen bonding with water) present near the polar headgroup region of amphiphilic molecules contributes to the headgroup hydration of liposomal aggregates.[25] With the covalent bond distance of the ester carbonyl group from the positively charged nitrogen in lipid **2** being shorter than that in lipid **1**, the degree of interfacial hydration is likely to be higher in lipid **2** liposomes. The enhanced interfacical hydration in lipid **2** liposomes, in turn, is expected to significantly shield the large Coulombic repulsion among the positively charged headgroups thereby imparting higher rigidity to the liposomal membrane (through more compact packing of the amphiphiles in the liposomal aggregates). Consistent with this supposition, the degree of interfacial hydration of the transfection efficient cationic *N*-(1-(2,3-dioleoyloxy)propyl)-*N*,*N*,*N*-trimethylammonium chloride (DOTAP)/cholesterol liposomes has indeed been shown to be lower than that of its transfection incompetent DOTAP/DOPE counterpart.[26] Significantly more positive surface potentials of lipid **1** lipoplexes compared to those for the lipid **2** lipoplexes across the entire lipid/DNA charge ratio 0.5:1−8:1 (Table 1B) is also likely to originate from possibly less hydrated and therefore less shielded positive surface charges of lipid **1**/cholesterol liposomes. An important issue deserves mention at this

(17) Bally, M. B.; Harvie, P.; Wong, F. M.; Kong, S.; Wasan, E. K.; Reimer, D. L. *Adv. Drug Delivery Rev.* **1999**, *38*, 291−315.
(18) Zabner, J.; Fasbender, A. J.; Moninger, T.; Poellinger, K. A.; Welsh, M. J. *J. Biol. Chem.* **1995**, *270*, 18997−19007.
(19) Friend, D. S.; Papahadjopoulos, D.; Debs, R. J. *Biochim. Biophys. Acta* **1996**, *1278*, 41−50.
(20) Xu, Y.; Szoka, F. C., Jr. *Biochemistry* **1996**, *35*, 5616−5623.
(21) Wang, L.; MacDonald, R. C. *Gene Ther.* **2004**, *11*, 1358−1362.
(22) Regelin, A. E.; Fankhaenel, S.; Gurtesch, L.; Prinz, C.; v. Kiedrowski, G.; Massing, U. *Biochim. Biophys. Acta* **2000**, *1464*, 151−164.
(23) Savva, M.; Chen, P.; Aljaberi, A.; Selvi, B.; Spelios, M. *Bioconjugate Chem.* **2005**, *16*, 1411−1422.
(24) Akao, T.; Osaki, T.; Ito, A.; Kunitake, T. *Bull. Chem. Soc. Jpn.* **1991**, *64*, 3677−3681.
(25) Hübner, W.; Blume, A. *Chem. Phys. Lipids.* **1998**, *96*, 99−123.
(26) Hirsch-Lerner, D.; Barenholz, Y. *Biochim. Biophys. Acta* **1999**, *1461*, 47−57.

point of discussion. The distribution of cholesterol among different cellular membranes is not uniform. At high concentrations, free cholesterol can self-associate and form domains (rafts) of condensed complexes of cholesterol and membrane phospholipids.[27] The existence of similar cholesterol domains is being proposed within the membranes of cationic liposomes containing high amounts of cholesterol.[28] Since the cationic liposomes of lipids **1** and **2** contain high amounts of cholesterol, the existence of such cholesterol domains in these liposomal membranes cannot be ruled out. In that case the remarkably higher biomembrane fusogenicity of the less rigid lipid **1**/cholesterol may also be related to the smoother cholesterol partitioning into the negatively charged biomembrane mimicking liposomal formulations. Koynova et al. has recently demonstrated that pronounced nonlamellar phase forming liposomal compositions of a cationic amphiphile with two asymmetric hydrocarbon chains, namely oleoyldecanoyl-ethylphosphatidylcholine (C18:1/C10-EPC), is likely to act as a dominant factor behind their high membrane fusogenic and high transfection properties compared to its structurally very similar saturated asymmetric counterpart stearoyldecanoyl-ethylphosphatidylcholine (C18:0/C10-EPC).[12] Clearly, similar biophysical investigations need to be undertaken in the future to understand whether the remarkably high fusogenic as well as high gene delivery efficacies of lipid **1**/Chol liposomes compared to lipid **2**/Chol liposomes also correlates with its enhanced nonlamellar phase forming properties when mixed with cellular membranes.

Conclusions

In the present investigation, toward addressing an hitherto unexplored issue in liposomal gene delivery, namely, the influence of linker orientation, we have designed and synthesized two structurally isomeric very similar cationic lipids **1** and **2** (Scheme 1) bearing the same hydrophobic tails and the same polar headgroups connected by the same ester (linker) group. The only structural difference between the cationic amphiphiles **1** and **2** is the opposite orientation of the linker ester functionality. While lipid **1** showed high efficacies in delivering reporter genes into multiple cultured mammalian cells including CHO, COS-1, HepG2, and A549, lipid **2** was found to be essentially incompetent in transferring genes into any of these cells. Findings in both transmission electron microscopic and dynamic laser light scattering studies revealed no significant size difference between the liposomes and the lipoplexes of lipids **1** and **2**. Confocal microscopic studies using lipoplexes containing fluorescently labeled plasmid DNA demonstrated a significantly higher cellular uptake of DNA complexed with lipid **1** liposomes. Results of fluorescence resonance energy transfer (FRET) studies using cationic liposomes of lipids **1** and **2** and biomembrane mimicking liposomal systems (DOPC/DOPE/DOPS/Chol) containing fluorescently labeled donor (NBD-PE) and acceptor (Rho-PE) lipids are consistent with the significantly higher biomembrane fusogenicity of lipid **1** liposomes. Studies on the thermotropic phase behaviors of the pure cationic liposomes of lipids **1** and **2** using the techniques of differential scanning calorimetry (DSC) and fluorescence anisotropy revealed significantly less membrane rigidity of the lipid **1** liposomes than that of the lipid **2** liposomes. Findings in the dye entrapment experiment are consistent with the significantly less membrane rigidity for the transfection efficient lipid **1**/cholesterol (1:1 mole ratio) liposomes. Enhanced biomembrane fusogenicity and the contrastingly high transfection property of lipid **1** liposomes presumably originate from the less rigid or more fluid character of the lipid **1** liposomal membranes compared to that of the lipid **2** liposomal membranes. Taken together, the present findings demonstrate for the first time that even as a minor structural variation linker orientation reversal in cationic amphiphiles can profoundly influence DNA-binding characteristics, membrane rigidity, membrane fusibility, cellular uptake, and consequently gene delivery efficacies of cationic liposomes.

Experimental Section

Materials and Methods. Mass spectral data were acquired by using a commercial LCQ ion trap mass spectrometer (ThermoFinnigan, SanJose, CA) equipped with an ESI source or micromass Quatro LC triple quadrapole mass spectrometer for ESI analysis. ^{1}H NMR spectra were recorded on a Varian FT 200 MHz or AV 300 MHz NMR spectrometer. 1-Tridecanol, *n*-tetradecanoic acid, *tert*-butyldimethylsilyl chloride, tetra-*n*-butylammonium fluoride (1 M solution in THF), and Amberlyst A-26 chloride ion exchange resin were purchased from Lancaster (Morecambe, U.K.). Column chromatography was performed with silica gel (Acme Synthetic Chemicals, India, 60−120 mesh). p-CMV-SPORT-β-gal plasmid was a generos gift from Dr. Nalam Madhusudhana Rao of the Centre for Cellular and Molecular Biology, Hyderabad, India. Cell culture media, fetal bovine serum, 3-(4,5-dimethylthiazol-2-yl)-2,5-diphenyltetrazolium bromide (MTT), polyethylene glycol 8000, *o*-nitrophenyl-β-D-galactopyranoside, *N*-methyl-*n*,*n*-diethanolamine, and cholesterol were purchased from Sigma-Aldrich, St. Louis, MO, U.S.A. NP-40, antibiotics, and agarose were procured from Hi-media, India. Unless otherwise stated all reagents were purchased from local commercial suppliers and were used without further purification. COS-1, CHO, HepG2, and A549 cells were procured from the National Centre for Cell Sciences (NCCS), Pune, India. Cells were grown at 37 °C in Dulbecco's modified Eagle's medium (DMEM) with 10% fetal bovine serum (FBS) in a humidified atomosphere containing 5% CO_2/95% air. Elemental analyses (C, H, N, Cl) for lipids **1** and **2** were carried out in VIMTA LABS, Hyderabad, Inida.

Syntheses of *N*,*N*-Di-[*O*-tetradecanoyl-2-hydroxyethyl]-*N*-hydroxyethyl-*N*-methylammonium Chloride (Lipid 1, Scheme 1A). Steps a and b. Synthesis of *N*,*N*-Di-[*O*-tetradecanoyl-2-hydroxyethyl]-*N*-Methyl Amine (I, Scheme 1A): In a 50 mL single neck round bottomed flask pyridine (2.7 mL, 33 mmol) was added at 0 °C to a solution of *n*-tetradecanonic acid (5 g, 22 mmol) in dry DCM. Thionyl chloride (2.4 mL, 33 mmol) was added to the reaction mixture at 0 °C, and the reaction mixture was stirred at room temperature for 2 h. The unreacted thionyl chloride and pyridine were removed on a rotavapor by repeated chasing with dry DCM and *N*-methyl-*N*,*N*-diethanolamine (1 g, 8.4 mmol) dissolved in dry DMF was added to the residue at 0 °C. The temperature was gradually raised to room temperature, and the reaction mixture was stirred at room temparature for an additional 6 h. The resulting hydrochloride salt was filtered and washed with 20 mL of dry ether. Finally recrystallization from 5:15 (v/v) methanol/ethylacetate afforded a pure hydrochloride salt intermediate. The recrystalized hydrochloride salt was stirred for 5 min in a DCM (25 mL)/1 M aqueous NaOH (10 mL) biphasic system. The organic layer was separated, dried over anhydrous sodium sulfate, filtered, and the filtrate was concentrated on a rotary evaporator. The residue upon chromatographic purification on a 60−120 mesh silica gel column using 2% methanol/$CHCl_3$ as eluent afforded the intermediate tertiary amine

(27) McConnell, H. M.; Radhakrishnan, A. *Biochim. Biophys. Acta* **2003**, *1610*, 159−173.
(28) Hungerford, G.; Baptista, A. L. F.; Coutinho, P. J. G.; Castanheira, E. M. S.; Oliveira, E. C. D. R. *J. Photochem. Photobiol. A* **2006**, *181*, 99−105.

N,*N*-di-[*O*-tetradecanoyl-2-hydroxyethyl]-*N*-methyl amine (**I**, Scheme 1A) as a white solid (1.55 g, 13% yield, $R_f = 0.6$, 5% methanol/$CHCl_3$).

^{1}H NMR (200 MHz, $CDCl_3$): δ ppm = 0.9 (t, 6H, $-(CH_2)-CH_3$), 1.2−1.4 (m, 40H, $-O-CO-CH_2-CH_2-(CH_2)_{10}-$), 1.6−1.7 (m, 4H, $-O-CO-CH_2-CH_2-(CH_2)_{10}-$), 2.2 (t, 4H, $-O-CO-CH_2-CH_2-(CH_2)_{10}-$), 2.35 (s, 3H, $H_3C-N-CH_2-CH_2-$), 2.65 (t, 4H, $-N-CH_2-CH_2-$), 4.1 (t, 4H, $N-CH_2-CH_2-O-CO-$). ESIMS *m*/*z*: 540 [M + 1$^+$] (calcd for $C_{33}H_{65}NO_4$, 100%).

Steps c and d. In a 25 mL round bottomed flask intermediate **I** prepared in step b above (0.5 g, 0.9 mmol) and 2-bromoethanol (0.2 g, 1.56 mmol) were stirred at 85 °C for 4 h. Crystallization from 20 mL of 1:4 (v/v) benzene/*n*-pentane followed by column chromatographic purification (using 60−120 mesh silica gel and 4% methanol/$CHCl_3$, v/v, as eluent) and chloride ion exchange on Amberlyst A-26 resin (with methanol as eluent) afforded pure lipid **1** (0.06 g, 11% yield, R_f = 0.4, 10% methanol/chloroform).

^{1}H NMR (300 MHz, $CDCl_3$): δ ppm = 0.9 (t, 6H, $-(CH_2)_{10}-CH_3$), 1.2−1.4 (m, 40H, $-O-CO-CH_2-CH_2-(CH_2)_{10}-$), 1.5−1.7 (m, 4H, $-O-CO-CH_2-CH_2-(CH_2)_{10}-$), 2.35 (t, 4H, $CH_3(HOCH_2-CH_2)N^+-(CH_2-CH_2-O-CO-CH_2-(CH_2)_{10}-CH_3)_2$, 3.25 (s, 3H, $CH_3(HOCH_2-CH_2)N^+(CH_2-CH_2-O-CO-CH_2-(CH_2)_{10}-CH_3)_2$), 3.5−4.0 (m, 8H, $CH_3(HOCH_2-CH_2)N^+(CH_2-CH_2-O-CO-CH_2-(CH_2)_{10}-CH_3)_2$), 4.45 (m, 4H, $CH_3(HOCH_2-CH_2)N^+(CH_2-CH_2-O-CO-CH_2-(CH_2)_{10}-CH_3)_2$). ESIMS *m*/*z*: 585 [M + 1$^+$] (calcd for $C_{35}H_{70}NO_5$, 100%).

Synthesis of *N*,*N*-Di-(2-(*n*-tridecyloxycarbonyl)ethyl)-*N*-methyl,*N*-(2-hydroxyethyl)ammonium Chloride (Lipid 2, Scheme 1B): Step e. Synthesis of *O*-*tert*-Butyl-dimethylsilyl-2-ethanolamine (II, Scheme 1B): A solution of 2-aminoethanol (0.5 g, 8.2 mmol) dissolved in 2 mL of dry DCM was transferred to a 50 mL two-neck round-bottom flask, and the solution was cooled to 0 °C. Imidazole (0.84 g, 12.3 mmol) dissolved in 3 mL of dry DCM was added to this cold solution at 0 °C. *tert*-Butyl-dimethylsilylchloride (1.85 g, 12.3 mmol) in 5 mL of DCM was added to the cold reaction mixture and stirred for 15 min at 0 °C. The temperature was gradually raised to room temperature, and stirring was continued for an additional 12 h. The reaction mixture was then diluted with $CHCl_3$ (100 mL) and washed with water (2 × 50 mL). The organic layer was separated, dried over anhydrous Na_2SO_4, and concentrated on a rotary evaporator. The residue, upon chromatographic purification on a 60−120 mesh size silica gel column using 2% methanol/chloroform (v/v) as the eluent, afforded the title compound as a light brown liquid (0.9 g, 64% yield, R_f = 0.6, 5% methanol/chloroform).

^{1}H NMR (200 MHz, $CDCl_3$): δ (ppm) = 0.1 (s, 6H, $-Si-(CH_3)_2$), 0.9 (s, 9H, $Si-C(CH_3)_3$), 2.7 (t, 2H, $H_2N-CH_2-CH_2-$), 3.6 (t, 2H, $CH_2-CH_2-O-Si-$).

Step f. Synthesis of *N*-2-*tert*-Butyl-dimethylsilyloxyethyl-*N*,*N*-di-(2-*n*-tridecyloxycarbonyl)ethyl Amine (III, Scheme 1B): A mixture of intermediate **II** prepared above in step e (0.15 g, 0.8 mmol), the bromo-ester intermediate V (0.71 g, 2.12 mmol, prepared as described below in step j), and K_2CO_3 (0.35 g, 2.55 mmol) in 5 mL of ethylacetate was taken in a 25 mL round-bottom flask, and the reaction mixture was stirred at 60 °C for 48 h. The reaction mixture was diluted with 50 mL of ethylacetate and washed with water (2 × 30 mL). The organic layer was separated, dried over anhydrous sodium sulfate, filtered, and concentrated on a rotavapor. The residue upon chromatographic purification using a 60−120 mesh size silica gel column and 5% ethylacetate/hexane, v/v, as eluent afforded the pure title compound as a colorless liquid (0.15 g, 25% yield, R_f = 0.4, 10:90 ethylacetate/hexane).

^{1}H NMR (200 MHz, $CDCl_3$): δ ppm = 0.1 (s, 6H, $-Si-(CH_3)_2-$), 0.9 (s and t, 15H, $Si-C(CH_3)_3$, $-CH_2-(CH_2)_{10}-CH_3$), 1.2−1.4 (m, 40H, $-CO-O-CH_2-CH_2-(CH_2)_{10}-CH_3$),1.6−1.7 (m, 4H, $-CO-O-CH_2-CH_2-(CH_2)_{10}-$), 2.45 (t, 4H, $N-(CH_2-CH_2-CO-O)$, 2.6 (t, 2H, $N-(CH_2-CH_2-OH)$, 2.85 (t, 4H, $N-CH_2-CH_2-CO-O$), 3.6 (t, 2H, $-N-CH_2-CH_2-$OTBDMS), 4.1 (t, 4H, $N-CH_2-CH_2-CO-O-CH_2-$).

Step g. Synthesis of *N*-2-Hydroxyethyl-*N*,*N*-di-(2-tridecyloxycarbonyl)ethylamine (IV, Scheme 1B). Compoud **III** (0.15 g) prepared in step f above was dissolved in 2 mL of THF at 0 °C in a 25 mL round bottomed flask, and 2 mL of tetra-*n*-butyl ammonium (TBAF, 1 M in THF) were added to the cold solution. The temperature of the reaction mixture was gradually raised to room temperature, and stirring at room temperature was continued for 6 h. The reaction mixture was concentrated on a rotavapor, and the residue was diluted with 50 mL of $CHCl_3$ and washed with water (2 × 25 mL). The organic layer was separated, dried over anhydrous sodium sulfate, filtered, and concentrated. The residue upon column chromatographic purification using a 60−12 mesh size silica gel column and 15−20% ethylacetate/hexane, v/v, as eluent afforded the pure title compound **IV** as a colorless liquid (50 mg, 55% yield, R_f = 0.5, 30% ethylacetate/hexane).

^{1}H NMR (200 MHz, $CDCl_3$): δ ppm = 0.9 (t, 6H, $-(CH_2)-CH_3$), 1.2−1.4 (m, 40H, $CO-O-CH_2-CH_2-(CH_2)_{10}-$), 1.6−1.7 (m, 4H, $CO-O-CH_2-CH_2-(CH_2)_{10}-$), 2.4−2.5 (t, 4H, $N(-CH_2-CH_2-CO-O-$), 2.6 (t, 2H, $-N-CH_2-CH_2-O-$), 2.8 (t, 4H, $-N-CH_2-CH_2-CO-O-$) 3.6 (t, 2H, $-N-CH_2-CH_2-O-$), 4.1 (t, 4H, $N(-CH_2-CH_2-CO-O-CH_2-$). ESIMS *m*/*z*: 570 [M + 1$^+$] (calcd for $C_{34}H_{67}NO_5$, 100%).

Steps h and i. Synthsis of *N*,*N*-di-(2-(*n*-tridecyloxycarbonyl)ethyl)-*N*-methyl,*N*-(2-hydroxyethyl)ammonium Chloride (Lipid 2, Scheme 1B): Intermediate **I**V (50 mg) prepared in step g above was dissolved in 1 mL of DCM in a 25 mL round-bottom flask, and 1 mL of methyl iodide was added to the solution. The reaction mixture was stirred at room temperature for 4 h and concentrated. Crystallization from 20 mL of 1:5 (v/v) ethylacetate/*n*-pentane followed by chloride ion exchange on Amberlyst A-26 resin (using chloroform as eluent) afforded pure lipid **2** as a white solid (0.04 g, 78% yield, R_f = 0.3, 5% methanol/chloroform).

^{1}H NMR (200 MHz, $CDCl_3$) : δ ppm = 0.9 (t, 6H, $-(CH_2)_{10}-CH_3$), 1.2−1.4 (m, 40H, $-CO-O-CH_2-CH_2-(CH_2)_{10}-$), 1.6−1.7 (m, 4H, $CO-O-CH_2-CH_2-(CH_2)_{10}-$), 2.9 (t, 4H, $N(-CH_2-CH_2-CO-O-$)), 3.4 (s, 3H, $H_3C-N^+-CH_2-CH_2-$), 3.8−3.9 (t, 2H, $-N^+-CH_2-CH_2-OH$), 4.1 (t, 4H, $N(-CH_2-CH_2-CO-O-CH_2-$). ESIMS *m*/*z*: 585 [M + 1$^+$] (calcd for $C_{35}H_{70}NO_5$, 100%).

Step j. Synthesis of *n*-Tridecyl-3-bromopropionate (Scheme 1C): A solution of 3-bromopropanoic acid (1 g, 6.5 mmol) in 5 mL of dry DCM was taken in a 50 mL single-neck round-bottom flask, and the solution was cooled to 0 °C. Sequentially pyridine (0.8 mL, 9.8 mmol) and thionyl chloride (0.8 mL, 9.8 mmol) were added to the cold solution at 0 °C. The temperature was gradually raised to room temperature, and the reaction mixture was stirred at room temperature for 2 h. The unreacted thionyl chloride and pyridine were removed on a rotavapor by repeated chasing with dry DCM, and *n*-tridecyl alcohol (1.6 g, 8.0 mmol) dissolved in 5 mL of dry DCM was added to the residue. The reaction mixture was stirred at room temperature for 6 h, diluted with 100 mL of $CHCl_3$, and washed with water (2 × 50 mL). The organic layer was separated, dried over anhydrous sodium sulfate, and concentrated by rotary evaporator. The residue, upon column chromatographic purification over 60−120 mesh size silica gel column using 2% ethylacetate/hexane (v/v) as eluent, afforded the pure title compound as a colorless liquid (1.2 g, 51% yield, R_f = 0.7, 10% ethylacetate/hexane).

^{1}H NMR (200 MHz, $CDCl_3$): δ (ppm) = 0.9 (t, 3H, $H_3C-CH_2-(CH_2)_{10}-$), 1.3−1.4 (m, 20H, $H_3C(-CH_2)_{10}-CH_2-$), 1.7 t, 2H, $-CH_2-CH_2-O-CO-$), 2.9 (t, 2H, $(-O-CO-CH_2-CH_2-$), 3.7 (t, 2H, $Br-CH_2-CH_2-$), 4.2 (t, $CH_2-CH_2-O-CO-$).

Preparation of Liposomes. The cationic lipid and cholesterol in the appropriate mole ratios were dissolved in a mixture of chloroform and methanol (3:1, v/v, 500 μL) in a glass vial. The solvent was removed with a thin flow of moisture-free nitrogen gas, and the dried lipid film was kept under high vacuum for 8 h. A 1 mL aliquot of sterile deionized water was added to the vacuum-dried lipid film, and the mixture was allowed to swell overnight. The vial was then vortexed

for 2−3 min at room temperature to produce multilamellar vesicles (MLVs). MLVs were then sonicated in an ice bath until clarity using a Branson 450 sonifier at 100% duty cycle and 25 W output power to produce small unilamellar vesicles (SUVs).

Plasmid DNA. *p*-CMV-SPORT-β-gal plasmid was amplified in DH5α-strain of *Escherichia coli*, isolated by alkaline lysis procedure and finally purified by PEG-8000 precipitation as described previously.[8a] The purity of plasmid was checked by A_{260}/A_{280} ratio (around 1.9) and 1% agarose gel electrophoresis.

Transfection of Cells. Cells were seeded at a density of 10 000 cells (for CHO and COS-1) and 15 000 cells (for A549 and HEPG2) per well in a 96-well plate 18−24 h before the transfection. A 0.3 μg amount of plasmid DNA was complexed with varying amounts of lipids (0.45−7.2 nmol) in a plain DMEM medium (total volume made up to 100 μL) for 30 min. The lipid/DNA (±) charge ratios were from 0.5:1 to 8:1 over these ranges of the lipids. The complexes were then added to the cells. After 3 h of incubation, DMEM was removed, and a 10% complete medium was added to the cells. The medium was changed with a 10% complete medium after 24 h, and the reporter gene activity was estimated after 48 h. The cells were washed with PBS (2 × 100 μL) and lysed with 50 μL of lysis buffer [0.25 M Tris-HCl pH 8.0, 0.5% NP40]. Care was taken to ensure complete lysis. The β-galactosidase activity per well was estimated by adding 50 μL of 2X-substrate solution [1.33 mg/mL of *o*-nitrophenyl-β-D-galactopyranoside (ONPG), 0.2 M sodium phosphate (pH 7.3), and 2 mM magnesium chloride] to the lysate in a 96-well plate. Absorption at 405 nm was converted to β-galactosidase units using a calibration curve constructed with pure commercial β-galactosidase enzyme. The values of β-galactosidase units in triplicate experiments assayed on the same day varied by less than 20%. The transfection experiment was carried out in duplicate, and the transfection efficiency values shown in Figure 1 are the average of triplicate experiments performed on the same day. The day-to-day variation in the average transfection efficiency was found to be within 2-fold. The transfection profiles obtained on different days were identical.

Toxicity assay. Cytotoxicities of the lipids **1** and **2** were assessed by the 3-(4,5-dimethylthiazol-2-yl)-2,5-diphenyltetrazolium bromide (MTT) reduction assay as described earlier.[10a] The cytotoxicity assay was performed in 96-well plates by maintaining the same ratio of number of cells to amount of cationic lipid, as used in the transfection experiments. MTT was added 3 h after addition of cationic lipid to the cells. Results were expressed as percent viability = [A_{540}(treated cells) − background/A_{540}(untreated cells) − background] × 100.

Zeta Potential (ξ) and Size Measurments. The sizes and the surface charges (zeta potentials) of liposomes and lipoplexes were measured by photon correlation spectroscopy and electrophoretic mobility on a Zeta sizer 3000HS_A (Malvern UK). The sizes were measured in deionized water with a sample refractive index of 1.59 and a viscosity of 0.89. The system was validated by using the 200 nm + 5 nm polystyrene polymer (Duke Scientific Corps. Palo Alto, CA). The diameters of liposomes and lipoplexes were calculated by using the automatic mode. The zeta potential was measured using the following parameters: viscosity, 0.89 cP; dielectric constant, 79; temperature, 25 °C; F(Ka), 1.50 (Smoluchowski); maximum voltage of the current, V. The system was validated by using DTS0050 standard from Malvern, U.K. Measurements were done 10 times with the zero-field correction. The potentials were calculated by using the Smoluchowski approximation.

DNA Binding Assay. The DNA binding ability of the cationic lipids **1** and **2** were assessed by their gel retardation assay on a 1% agarose gel (prestained with ethydium bromide) across the varying lipid/DNA charge ratios of 0.5:1 to 8:1. pCMV-β-gal (0.30 μg) was complexed with the varying amount of cationic lipids in a total volume of 20 μL in Hepes buffer, pH 7.40, and incubated at room temperature for 20−25 min. A 4 μL aliquot of 6X loading buffer (0.25% Bromophenol blue in 40% (w/v) sucrose in H_2O) was added to it, and the resulting solution (24 μL) was loaded on each well. The samples were electrophoresed at 80 V for 45 min, and the DNA bands were visualized in the gel documentation unit.

DNase I Sensitivity Assay. Briefly, in a typical assay, pCMV-SPORT-β-gal plasmid (1 μg) was complexed with a varying amount of cationic lipids in a total volume of 30 μL in Hepes buffer, pH 7.40, and incubated at room temperature for 30 min on a rotary shaker. Subsequently, the complexes were treated with 10 μL of DNase I (at a final concentration of 1 μg/mL) in the presence of 20 mM $MgCl_2$ and incubated for 20 min at 37 °C. The reactions were then halted by adding EDTA (to a final concentration of 50 mM) and incubated at 60 °C for 10 min in a water bath. The aqueous layer was washed with 50 μL of phenol/chloroform/isoamylalcohol (25:24:1mixture, v/v) and centrifuged at 10 000 g for 5 min. The aqueous supernatants were separated, loaded (20 μL) on a 1% agarose gel (prestained with ethydium bromide), and electrophoresed at 100 V for 1 h.

Transmission Electron Microscopy. Transmission electron microscopy was performed on a FEI Tecnai 12 TEM apparatus operated at 100 kV. Lipoplex samples were transferred onto an ultrathin-carbon coated copper grid by placing the grid on top of a 10 μL drop of the sample for 1 min. After removing the excess fluid from one side, the grid was placed on a 20 μL water drop for a 30 s wash. The excess fluid was removed, and the grid was placed for 1 min on a 20 μL drop of freshly filtered uranyl acetate (1.33%). Once again, the excess fluid was wicked away, and the grid was air-dried.

DNA Uptake Study by Confocal Microscopy: For confocal microscopy experiments, 100 000 cells were seeded in each well of a 24-well plate and cells were incubated with lipoplexes (with 1:1 lipid/DNA charge ratio) of lipids **1** and **2** in 200 μL of DMEM containing 25 μg of fluorescein-labeled p-CMV-SPORT-β-gal plasmid DNA (prepared by "random primed" fluoroscein-12-dUTP labeling of p-CMV-SPORT-β-Gal following the manufacturer's instructions available with Roche's Fluoroscein High Prime Kit, Catalog No. 1 585 622) for 4 h at 37 °C. DMEM was removed, and the cells were washed with PBS (2 × 200 μL) and trypsinized with 0.1% Trypsin/EDTA solution. A 500 μL aliquot of complete medium was added to the trypsinized cell suspension, the suspension ws centrifuged for 3 min at 2000 rpm, and the complete medium was removed. PBS (500 μL) was added to the cells, and the cell suspension was once more centrifuged for 3 min at 2000 rpm. The supernatant was removed, and the cell pellets were resuspended in 500 μL of PBS. A 20 μL aliquot of this cell suspension was applied to a glass slide, a cover slip was put on the cells on the glass slide, and the slide was then mounted onto the confocal microscope (Leica TCS SP2 organic laser scanner) at a 200 magnification. The cells containing fluorescein-labeld DNA were then viewed using the 488 nm excitation line of krypton/argon laser, and the green fluorescences were detected at 514−550 nm.

FRET Assay. The membrane fusion activity of both Chol/lipid **1** (1:1 mole ratio) and Chol/lipid **2** (1:1 mole ratio) liposomes were measured with the FRET assay essentially as described previously.[12] NBD-PE and Rho-PE (Avanti-Polar Lipids, USA) were used as the donor and acceptor fluorescent lipids, respectively. The liposome DOPC/DOPE/DOPS/Chol (45:20:20:15, w/w ratio, the total lipid concentration used was 0.5 mM) was used as the biomembrane mimicking lipid formulation, and this liposomal formulation was labeled with the donor and acceptor lipids. The concentrations of both donor and acceptor lipids were 0.005 mM (i.e., 1% with respect to the total biomembrane mimicking lipid content). The total lipid concentrations used in both the Chol/lipid **1** (1:1 mole ratio) and Chol/lipid **2** (1:1 mole ratio) liposomes were the same as those of the biomembrane micking lipid formulation (0.5 mM). Labeled model biomembrane liposomal formulations were placed in an FL_X 800 Microplate Fluoroscence Reader (BioTek Instruments Inc., U.K.) at room temperature, and equimolar amounts of Chol/lipid **1** (1:1 mole ratio) and Chol/lipid **2** (1:1 mole ratio) liposomes were added. Fluorescence intensities were recorded as a function of time with excitation at 485 nm and emission

at 595 nm. Fusion (100%) was determined from the Rho-PE fluorescence intensity of the labeled biomembrane liposomal formulation in the presence of 1% Triton X100.

Differential Scanning Calorimetry. Lipids **1** and **2** (2.2 mg) were dissolved in 150 μL of choloroform, and the solvent was removed by chasing with a gentle flow of dry N_2 gas. The residual solvent was removed under high vacuum for 6−8 h. The dry lipid films were hydrated with 250 μL of pure deionized water at room temperature overnight, vortexed, and sonicated to clarity in a bath sonicator (ULTRAsonik 28X). Differential scanning calorimetry (DSC) experiments with the resulting liposomal samples (50 μL of liposomes containing 0.43 mg of lipids) were performed on an 821^e Mettler-Toledo (Schwerzenbach, Switzerland) calorimeter. Sealed aluminum crucibles of 50 μL capacity were used as sample holders. The scan rates for heating were 5 °C/min. Thermograms were obtained between 0 and 70 °C and were referenced against deionized water.

Fluorescence Anisotropy Measurements. Lipids **1** and **2** (0.58 mg) were dissolved in 100 μL of choloroform along with DPH at a lipid/DPH mole ratio of 300:1 and dried under a gentle flow of dry N_2 gas. The residual solvent was removed under high vacuum for 6−8 h. The dried lipid films were hydrated in 1 mL of buffer (Tris-HCl, pH 7.4, 100 mM) overnight, vortexed, and sonicated to clarity in a bath sonicator (ULTRAsonik 28X). The resulting liposomal solutions were used for anisotropy measurements. Anisotropy was measured by recording the DPH fluorescence values (excitation at 354 nm and emission at 427 nm) in parallel and perpendicular polarizer positions in a Fluorolog 3-22 fluorescence spectrophotometer. The fluorescence intensity of the emitted light polarized parallel ($I_{||}$) and perpendicular ($I_{\perp}$) to the excited light across the temperature range 15−60 °C (scan rate 5 °C/min, the samples were allowed to equilibrate for 5 min between the successive scans). The fluorescence anisotropy values (r) were calculated by the instrument software using the Perrin equation $r = (I_{||}) - (GI_{\perp})/(I_{||}) + (GI_{\perp})$ where G is the instrumental grating factor.

Dye Entrapment Experiment. The protocols followed for liposomal entrapment of 5/6-CF and for monitoring its subsequent release from the liposomes were essentially as described previously.[29] Briefly, equimolar cholesterol containing liposomal suspensions of lipids **1** and **2** (1 mM total lipid concentration; 0.5 mM in both cationic lipid and cholesterol) were prepared in Tris-HCl buffer (25 mM, pH 8.0) containing 25 mM CF. The CF-loaded liposomes were separated from the unentrapped free CF dye by passing through a sephadex G-50 column with an elution buffer of 50 mM Tris-HCl buffer (pH 8.0). Transmembrane permeation of the liposomally loaded CF was measured at 25 °C by following the changes in fluorescence intensity of the emitted light (due to leakage of CF from liposomes) in 60 min in an FL_X 800 Microplate Fluoroscence Reader (BioTek Instruments Inc., U.K.). The excitation and emission wavelengths used for this experiment were 485 and 528 nm, respectively. Percentage CF releases were calculated using the equation: Permeation of CF (%) = $[(F_t - F_i)/(F_f - F_i)] \times 100$ where F_i, F_t, and F_f are the fluorescence emission values at time $t = 0$, at time t, and the final fluorescence on complete disruption of liposomal structures with the final concentration of 1% (v/v) Triton X-100.

(29) Bhattacharya, S.; Haldar, S. *Biochim. Biophys. Acta* **2000**, *1467*, 39−53.

Acknowledgment. Financial support received from the Department of Biotechnology, Government of India (to A.C.) is gratefully acknowledged. M.R. thanks the Council of Scientific and Industrial Research (CSIR), Government of India, for his doctoral research fellowship; J.S. and K.M. thank the University Grant Commission, Government of India, for their doctoral research fellowships. We sincerely thank Dr. Anand K. Kondapi and Mr. A. D. Saikrishna, University of Hyderabad, for their help in conducting the confocal microscopic experiments in their laboratory. We gratefully acknowledge the help from Dr. N. M. Rao and Mr. Shoeb Ahmed, Centre for Cellular and Molecular Biology, in taking fluorescence anisotropy measurements in their laboratory.

Note Added after ASAP Publication. After this paper was published ASAP on August 25, 2007, an error was corrected in the heading for Scheme 1C. The corrected version was published ASAP on August 31, 2007.

Supporting Information Available: ^{1}H NMR (200 MHz) spectra of all the synthetic intermediates shown in Scheme 1 as well as those of final target lipids **1** and **2**, ESI mass spectra for the final lipids **1** and **2**, reversed phase HPLC chromatograms for lipids **1** and **2** in two mobile phases and the details of the HPLC conditions, TEM pictures of liposomes and lipoplexes, percent cell viability data, epifluorescence micrographs for cellular uptake experiments using labeled liposomes, FRET results based on increasing NBD fluorescence, percent CF leakage data in dye entrapment experiments, and elemental analysis data for lipids **1** and **2**. This material is available free of charge via the Internet at http://pubs.acs.org.

JA0704683